Wave Formation on a Vertical Falling Liquid Film

The method of integral relations is used to derive a nonlinear two-wave equation for long waves on the surface of vertical falling liquid films. This equation is valid within a range of moderate Reynolds numbers and can be reduced in some cases to other well-known equations.

The theoretical results for the fastest growing waves are compared with the experimental results concerning velocities, wave numbers, and growth rates of the waves in the inception region. The validity of the theoretical assumptions is also confirmed by direct measurements of instantaneous velocity profiles in a wave liquid film.

The results of the experimental investigation concerning nonlinear stationary waves and the evolution of initial solitary disturbances are presented.

S. V. ALEKSEENKO,
V. Ye. NAKORYAKOV and
B. G. POKUSAEV

Institute of Thermophysics
Siberian Branch,
USSR Academy of Sciences,
Novosibirsk-90, 630090, U.S.S.R.

SCOPE

Vertical falling liquid films are extensively used in interphase heat and mass transfer processes in chemical technology and energetics. It is well known that on the surface of these films there practically always exist waves that can influence the transfer processes. In the case of short test sections and moderate liquid flow rates these waves are ordered and two-dimensional. To estimate the transfer coefficients for the wave flows of films one should be able to calculate the nonlinear wave regimes, because it is the nonlinear waves that are dominating in wave formation on the surface of the above films.

Most known publications on nonlinear waves are devoted to calculations of either nonstationary or stationary waves at low and moderate flow rates, respectively. However, there is no general-purpose nonlinear, nonstationary equation which would generalize the available approaches and be valid in a wide range of conditions. The aim of the present study has been to derive a general-purpose model equation for nonlinear, nonstationary waves on the film surface and to substantiate the validity of this approach on the basis of the existing experimental data and theoretical results.

CONCLUSIONS AND SIGNIFICANCE

A universal model equation to describe nonlinear, nonstationary waves on the surface of liquid films in the range of Re numbers $1 \leq Re \leq \epsilon^{-2}$ (ϵ is the long-wave process parameter) is derived by the method of integral relations by using self-similar velocity profiles. The equation has a two-wave structure, which implies that at low $Re(\sim 1)$, kinematic waves can be observed, to which the energy is transferred by means of a higher-order wave mechanism. At $Re \sim 1/\epsilon^2 \gg 1$, the higher-order waves grow at the expense of the kinematic waves. In the limiting cases of low and high Re numbers and in the particular case of stationary waves, the above two-wave equation can be reduced to the well-known equations of Gjevik (1970), Nakoryakov and Shreiber (1973), and Shkadov (1967).

In terms of the derived equation, a linear analysis of the stability has been carried out. Analytical expressions to describe neutral disturbances, the fastest growing waves, and capillary ripples observed in front of the large solitary waves have been obtained.

An experimental setup has been developed to measure the instantaneous velocity profiles in a wave liquid film and the wave characteristics in the region of their formation. The assumed validity concerning the self-similarity of the instantaneous velocity profiles has been corroborated by the data on the instantaneous velocity field in a film for two-dimensional, moderate-amplitude waves.

The data on the wave characteristics in the region of wave formation have been generalized in the universal coordinates obtained from the analysis of the above two-wave equation. It has been shown that the behavior of linear growing waves on the film surface can be described by the linear theories of the fastest growing waves. The calculations carried out according to these equations are in good agreement with the other known theories in a wide range of the $Re/Fi^{1/11}$ values, apart from very high Re numbers.

The results of the experimental investigation of nonlinear stationary periodic waves and the evolution of initial solitary disturbances are presented. Various types of two-dimensional waves have been discovered.

The results provide hope that the solutions of the full two-wave equations will describe all the two-dimensional nonlinear wave regimes observed on the surface of falling liquid films.

INTRODUCTION

The stability of vertical falling liquid films was studied in terms of the Orr-Sommerfeld equation by Benjamin (1957), Yih (1963), Whitaker (1964), and Krantz and Goren (1971). Kapitza (1948), Shkadov (1967, 1968), Krylov et al. (1969), and Lee (1969) performed such an analysis on the basis of the boundary layer equations.

The dependencies of the growth rate and of the phase velocity of waves have been obtained, the neutral curves have been plotted, and the characteristics of the fastest growing waves have been calculated.

Despite the fact that vertical falling films are unstable, the experiments point to the existence of stationary wave movement, the amplitude of the waves being constant. The finite-amplitude wave flow can be analyzed in terms of nonlinear equations only. It is very convenient to perform such an analysis by using one equation, e.g., for the film thickness, the flow rate, or the flow velocity.

The nonlinear wave studies are conditionally subdivided into two groups in which low ($Re \sim 1$) and high ($Re \lesssim 400$) Reynolds numbers, respectively, are considered for the laminar wave film flow regime alone.

Kapitza (1948) was the first to analyze film surface stationary waves at moderate Reynolds numbers. His approach is based on the boundary-layer-type equations, as well as on the method of integral relations. The finite equation actually represents an equation for the theory of long capillary waves on shallow water, written for the case of neutral waves. As a matter of fact, Kapitza found a condition when neutral wave regimes (i.e., those that are neither growing nor damped) exist, and obtained expressions for the velocity and the length of neutral waves propagating on a film. He also tried to predict the equilibrium wave amplitude from the balance between the energy dissipation rate and the gravitational work, as well as from an additional hypothesis concerning the minimum dissipation function for the actual wave flow regime. This theory does not appear to be rigorous in many respects. To a considerable extent it is based on physical arguments rather than on a strict derivation.

The paper by Kapitza resulted in many contributions by his followers, among whom one should mention Shkadov (1967, 1968, 1973) and Lee (1969) particularly. Shkadov studied nonlinear stationary waves at moderate Reynolds numbers ($Re \sim 30$) also on the basis of the boundary-layer-type equations for long waves and of the method of integral relations. Periodic solutions were found as expansions in harmonics. Having retained the first two harmonics in the solution, Shkadov showed that using additional harmonic amplitude equations and a minimum film thickness hypothesis, similar to that proposed by Kapitza, enables us to calculate all the basic wave characteristics, including amplitude. The nonlinearity of the process manifests itself both in deviation of the waveform from the harmonic one and in alteration of the mean film thickness. A similar study was performed by Lee (1969), who solved the problem of stationary nonlinear waves on the basis of Kapitza's equations by using the Bogolyubov-Krylov method.

Thus, all the research dealing with the analysis of nonlinear wave regimes at moderate Reynolds numbers has been performed on the basis of Kapitza's equations obtained as a boundary layer approximation. The dynamic and continuity equations are reduced to one equation on the assumption that the waves are stationary and the solution is a simple wave.

Beginning with Ivanilov's study (1961), the "narrow bands" method consisting in an expansion of the solution in h/λ powers, where h is the film thickness and λ the wavelength, is used to analyze long waves at low Reynolds numbers. Since the equations comprise the products h/λ. Re, the condition $Re \sim 1$ is necessary to insure the convergence of the expansion.

Some long-wave theory equations of various degrees of accuracy were obtained from the complete system of the Navier-Stokes equations by Ivanilov (1961), Benney (1966), Pashinina (1966), Gjevik (1970), and Maurin et al. (1977). Detailed analysis of the solutions and of their stability is given by Nepomnyshchii (1974, 1977). Petviashvili and Tzvelodub (1978) and Tzvelodub (1980) obtained solutions both for stationary periodic waves and stationary two- and three-dimensional solitons on a liquid film at $Re \sim 1$. A typical equation of the above-mentioned theories for the case of low Re numbers turns out to be nonstationary, being of the fourth order along a coordinate and containing the second derivative, responsible for the instability of the smooth flow.

Thus the present situation in the theory is as follows. The flow stability has been studied on the basis of the Orr-Sommerfeld equation, as well as on the basis of the boundary layer equations. The nonlinear wave motion at low Re numbers has been analyzed by means of the Benney-Gjevik-type equation which allows us to investigate both the nonstationary effects and the stationary wave solutions.

For moderate Re numbers no model equation of this type is known. There exist only those of the Kapitza-type equations that are suitable for the analysis of stationary wave regimes. One attempt to obtain a model equation for high Re numbers was made by Nakoryakov and Shreiber (1973).

There is a certain objective necessity to derive a general-purpose nonstationary, nonlinear wave equation which would make it possible to generalize the existing approaches. One may formulate a priori the requirements which should be met by these equations. It should insure the analysis of stability and be reduced to the Benney-Gjevik equation at low Re numbers. In the stationary case, it should coincide with the Kapitza-type equation and at high Re numbers be reduced to the Nakoryakov and Shreiber equation (1973). An attempt to derive such an equation is reported in the present paper.

As far as the experimental studies are concerned, only a few publications whose results may be compared with the theoretical models should be mentioned. These are the papers by Kapitza and Kapitza (1949), Jones and Whitaker (1966), Strobel and Whitaker (1969), Krantz and Goren (1971), Portalski and Clegg (1972), Pierson and Whitaker (1977) and Nakoryakov et al. (1975, 1976, 1977). This is due to the fact that the film wave theory has been fairly well developed only for two-dimensional periodic waves of small amplitude and of almost sinusoidal form. In practice, the two-dimensional regular wave regimes are usually observed at $Re \approx 5$–20, near the wave inception line. In all the other cases the film waves turn out to be three-dimensional and irregular, and their form may noticeably differ from the sinusoidal one. Therefore, almost all the experimental studies actually resolve themselves into statistical analyses of wave characteristics without two- and three-dimensional, stationary and nonstationary waves being separated. This information surely cannot provide complete verification of the theoretical models nor help us discover the physical regularities of wave motion.

In the above experimental studies it turned out to be possible to investigate the two-dimensional regular wave regimes either near the wave inception line within a limited range of variations in flow rates, properties of liquids, and wave characteristics, or using the artificial regularization method (superposition of external disturbances). To verify the stability theories, Krantz and Goren (1971) excited waves by wire vibrations at the initial film section. In the paper by Kapitza and Kapitza (1949), as well as in our research, the stationary wave regimes were mainly studied via wave excitation by pulsations of the liquid flow rate.

The experiments dealing with the investigation of waves in the inception region show that the behavior of natural growing waves can be described by the linear theories of the fastest growing waves. The majority of the studies, however, provide us with data for velocity and wave number only, often without mentioning that it

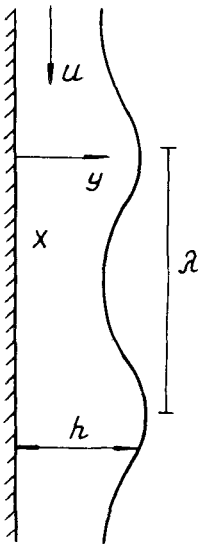

Figure 1. Schematic representation of a vertical falling liquid film.

is the two-dimensional flow that is under study. The theories of steady finite amplitude waves are in agreement with the experimental results for almost sinusoidal waves within the range of numbers $Re \lesssim 20$.

Experimental data on instantaneous velocity profiles in a wave liquid film are completely absent from the literature, although such measurements are considered to be of extreme importance, since many theories utilize various velocity distribution hypotheses. This paper presents experimental data of wave characteristics and of instantaneous velocity profiles for strictly two-dimensional waves only.

DERIVATION OF THE WAVE EQUATION

Let the Navier-Stokes equations and the boundary conditions for a vertical falling liquid film (Figure 1) be written in the dimensionless form

$$\frac{\partial \bar{u}}{\partial \bar{t}} + \bar{u}\frac{\partial \bar{u}}{\partial \bar{x}} + v\frac{\partial \bar{u}}{\partial \bar{y}} = \frac{3}{\epsilon \cdot Re} + \frac{1}{\epsilon \cdot Re}\left(\frac{\partial^2 \bar{u}}{\partial \bar{x}^2}\cdot \epsilon^2 + \frac{\partial^2 \bar{u}}{\partial \bar{y}^2}\right) - \frac{\partial \bar{P}}{\partial \bar{x}} \quad (1)$$

$$\epsilon^2\left(\frac{\partial \bar{v}}{\partial \bar{t}} + \bar{u}\frac{\partial \bar{v}}{\partial \bar{x}} + \bar{v}\frac{\partial \bar{v}}{\partial \bar{y}}\right) = \frac{\epsilon}{Re}\frac{\partial^2 \bar{v}}{\partial \bar{y}^2} + \frac{\epsilon^3}{Re}\frac{\partial^2 \bar{v}}{\partial \bar{x}^2} - \frac{\partial \bar{P}}{\partial \bar{y}} \quad (2)$$

$$\partial \bar{u}/\partial \bar{x} + \partial \bar{v}/\partial \bar{y} = 0 \quad (3)$$

at $y = h$,

$$\epsilon^2 \frac{4\partial \bar{h}/\partial \bar{x}}{1 - \epsilon^2(\partial \bar{h}/\partial \bar{x})^2}\cdot\frac{\partial \bar{v}}{\partial \bar{y}} + \frac{\partial \bar{u}}{\partial \bar{y}} + \epsilon^2\frac{\partial \bar{v}}{\partial \bar{x}} = 0 \quad (4)$$

$$\bar{P} - P_o = -\frac{3^{1/3}Fi^{1/3}\epsilon^2}{Re^{5/3}}\frac{\partial^2 \bar{h}/\partial \bar{x}^2}{[1 + \epsilon^2(\partial \bar{h}/\partial \bar{x})^2]^{3/2}} + \frac{2\epsilon}{Re}\frac{\partial \bar{v}}{\partial \bar{y}}\left[\frac{1 + \epsilon^2(\partial \bar{h}/\partial \bar{x})^2}{1 - \epsilon^2(\partial \bar{h}/\partial \bar{x})^2}\right] \quad (5)$$

at $y = 0$,

$$\bar{u} = 0, \bar{v} = 0 \quad (6)$$

at $y = h$,

$$\bar{v} = \frac{\partial \bar{h}}{\partial \bar{t}} + \bar{U}\frac{\partial \bar{h}}{\partial \bar{x}} \quad (7)$$

where $\bar{U}$ is the dimensionless longitudinal velocity component for the film surface.

The conditions in Eqs. 4 and 5 mean the absence of the tangential and normal stresses from the film surface, Eq. 7 being a common kinematic boundary condition on a free surface. Here the following dimensionless values have been introduced, i.e.,

$$\bar{u} = u/u_o, \bar{v} = (v/u_o)\cdot L/h_o, \bar{x} = x/L, \bar{y} = y/h_o$$

$$\bar{t} = tu_o/L, \bar{P} = P(\rho u_o^2), \epsilon = h_o/L, Re = q_o/\nu$$

and the film number $Fi = \sigma^3/(\rho^3 g\nu^4)$, where t is the time, L the characteristic longitudinal scale whose order is the same as with the wavelength λ, P the pressure, P_o the atmospheric pressure, q_o the volume liquid flow rate per unit widt, g the free fall acceleration, ν the kinematic viscosity, ρ the density, σ the liquid surface tension, and h_o and U_o can be determined from the Nusselt formulae for a smooth laminar film flow

$$Re = q_o/\nu = gh_o^3/(3\nu^2) = h_o u_o/\nu$$

Let a long-wavelength process be considered, provided that $\epsilon \ll 1$ and $Re \sim 1/\epsilon \gg 1$. Let the disturbed part U' of the longitudinal velocity U be separated, assuming that $U' \sim \epsilon_1 U_o$, $\epsilon_1 \sim \epsilon$. In so doing, having retained the terms of orders 1 and ϵ in Eqs. 1-7, we arrive at the boundary layer type equations which can be written in the dimensional form, i.e.,

$$\frac{\partial u}{\partial t} + u\frac{\partial u}{\partial x} + v\frac{\partial u}{\partial y} = \nu\frac{\partial^2 u}{\partial y^2} + g - \frac{1}{\rho}\frac{\partial P}{\partial x} \quad (8)$$

$$\frac{\partial u}{\partial x} + \frac{\partial v}{\partial y} = 0 \quad (9)$$

$$\partial P/\partial y = 0 \quad (10)$$

the boundary conditions being as follows:
at $y = h$,

$$v = \frac{\partial h}{\partial t} + U\frac{\partial h}{\partial x} \quad (11)$$

$$\partial u/\partial y = 0 \quad (12)$$

at $y = 0$,

$$u = v = 0 \quad (13)$$

at $y = h$,

$$P - P_o = -\sigma\cdot\partial^2 h/\partial x^2 \quad (14)$$

While deriving the system of Eqs. 8-14, it was taken into consideration that for real liquids, $Fi^{1/3}$ is high (e.g., for water, $Fi^{1/3} \approx 10^4$).

It should be noted that with the properly chosen relation between ϵ and ϵ_1, the final system of Eqs. 8-14 remains the same within the range of Reynolds numbers $1 \le Re \le \epsilon^{-2}$.

The method of integral relations (the Karman-Polhausen method) is used below. Its main disadvantage is that the film instantaneous velocity profile should be specified a priori. It is difficult to estimate its possible error, although it seems to be evident that it cannot be too high for long waves. The experimental results concerning the direct determination of instantaneous velocity profiles in a wavew liquid film (partially given in the present paper) testify to a fair approximation to the velocity profile by a self-similar polynomial for two-dimensional waves, at least, of moderate amplitude.

Integrating Eqs. 8 and 9 over the film thickness by using expressions 10-14 and considering that $h = h(x,t)$, we have

$$\frac{\partial}{\partial t}\int_0^h u dy + \frac{\partial}{\partial x}\int_0^h u^2 dy = -\nu\left(\frac{\partial u}{\partial y}\right)_{y=0} + gh + \frac{\sigma h}{\rho}\frac{\partial^3 h}{\partial x^3} \quad (15)$$

$$\frac{\partial h}{\partial t} + \frac{\partial}{\partial x}\int_0^h u dy = 0 \quad (16)$$

Such a system has been obtained in a number of papers, but unlike that research our objective consists in deriving one nonlinear, nonstationary equation for the film thickness disturbance.

Following the method of integral relations and resting on our own experimental results, let the velocity profile be presented as

$$u = U \cdot f(\eta),\ \eta = y/h$$

Now we introduce the instantaneous liquid flow rate in a film and express it as a function of f:

$$q = \int_0^h u dy = Uh \int_0^1 f d\eta$$

In a similar way, we have

$$\int_0^h u^2 dy = U^2 h \int_0^1 f^2(\eta) d\eta,\ \left(\frac{\partial u}{\partial y}\right)_{y=0} = \frac{U}{h} f'(0)$$

Using these expressions and introducing the coefficients

$$\int_0^1 f(\eta)d\eta = \delta,\ \int_0^1 f^2(\eta)d\eta = \gamma,\ f'(0) = æ,\ \chi = \gamma/\delta^2$$

we rewrite 15 and 16 as the thickness and the flow rate equations:

$$\frac{\partial q}{\partial t} + 2\chi\frac{q}{h}\frac{\partial q}{\partial x} - \chi\frac{q^2}{h^2}\frac{\partial h}{\partial x} = -\frac{æ\nu}{\delta}\frac{q}{h^2} + gh + \frac{\sigma h}{\rho}\frac{\partial^3 h}{\partial x^3} \quad (17)$$

$$\frac{\partial h}{\partial t} + \frac{\partial q}{\partial x} = 0 \quad (18)$$

We represent the overall flow as

$$q = q_o + q',\ h = h_o + h', \quad (19)$$

where prime denotes the disturbed part of the value, and substitute these expressions into Eqs. 17 and 18. Assuming that $q' \ll q_o, h' \ll h_o$ and retaining those terms of the equations whose order is $(h')^2, (q')^2$ or higher, we obtain nonlinear equations for the thickness and flow rate disturbances, the nonlinear terms being on the righthand side:

$$\frac{\partial q'}{\partial t} + \frac{2\chi q_o}{h_o}\frac{\partial q'}{\partial x} - \chi\frac{q_o^2}{h_o^2}\frac{\partial h'}{\partial x} + \frac{æ\nu}{\delta h_o^2}q' - 3gh' - \frac{\sigma h_o}{\rho}\frac{\partial^3 h'}{\partial x^3}$$
$$= \frac{3gh'^2}{h_o} - \frac{2h'}{h_o}\frac{\partial q'}{\partial t} - \frac{2\chi q_o}{h_o^2}\left[h'\frac{\partial q'}{\partial x} + \frac{h_o}{q_o}q'\frac{\partial q'}{\partial x} - q'\frac{\partial h'}{\partial x}\right] \quad (20)$$

$$\partial h'/\partial t + \partial q'/\partial x = 0 \quad (21)$$

Now we pass from the system of Eqs. 21 and 22 to one nonstationary equation for thickness disturbances. With this end in view, let Eq. 20 be differentiated with respect to x and the derivative $\partial q'/\partial x$ in the linear terms be replaced via the continuity equation Eq. 21:

$$\frac{\partial^2 h'}{\partial t^2} + \frac{2\chi q_o}{h_o}\frac{\partial^2 h'}{\partial x \partial t} + \chi\frac{q_o^2}{h_o^2}\frac{\partial^2 h'}{\partial x^2} + \frac{æ\nu}{\delta h_o^2}\frac{\partial h'}{\partial t} + 3g\frac{\partial h'}{\partial x}$$
$$+ \frac{\sigma h_o}{\rho}\frac{\partial^4 h'}{\partial x^4} = -\frac{6g}{h_o}h'\frac{\partial h'}{\partial x} + \frac{2}{h_o}\frac{\partial}{\partial x}\left(h'\frac{\partial q'}{\partial t}\right)$$
$$+ \frac{2\chi q_o}{h_o^2}\frac{\partial}{\partial x}\left[h'\frac{\partial q'}{\partial x} + \frac{h_o}{q_o}q'\frac{\partial q'}{\partial x} - q'\frac{\partial h'}{\partial x}\right] \quad (22)$$

To exclude q' and $\partial q'/\partial t$ from the nonlinear terms, the following considerations will be used. Let the variables x and t in the continuity equation be substituted by ξ and t, where $\xi = x\text{-}ct$ and c is the wave velocity assumed to be constant for the case of quasistationary waves. As follows from the experiments (see, for instance, Figures 9 and 10), in many cases the observed waves may be considered as weak-dispersive and weak-nonlinear. Then

$$\frac{\partial h'}{\partial t} - c\frac{\partial h'}{\partial \xi} + \frac{\partial q'}{\partial \xi} = 0 \quad (23)$$

In the case of the quasistationary process, the wave profile in a moving coordinate system deforms only slightly. As a result, we pass from Eq. 23 to the approximate equation $c\partial h'/\partial\xi = \partial q'/\partial\xi$, from which the relations

$$q' = ch' \quad (24)$$

$$\frac{\partial}{\partial t} = -c\frac{\partial}{\partial x} \quad (25)$$

follow. In the case of stationary waves, expressions 24 and 25 turn out to be exact.

Now substitute Eq. 24 into the nonlinear terms of Eq. 22, which at $1 \le Re \le \epsilon^{-2}$ are always on a lower order of magnitude than the main terms. The derivatives of the form $c\partial/\partial x$ that have appeared in the nonlinear terms will be substituted according to Eq. 25. As a result, we obtain the following nonlinear, nonstationary equation for the case of the thickness disturbances:

$$\left(\frac{\partial}{\partial t} + c_o\frac{\partial}{\partial x}\right)h' + \frac{\delta}{æ}\frac{h_o^2}{\nu}\left(\frac{\partial}{\partial t} + c_1\frac{\partial}{\partial x}\right)\left(\frac{\partial}{\partial t} + c_2\frac{\partial}{\partial x}\right)h'$$
$$+ 6g\frac{\delta h_o}{æ\nu}h'\frac{\partial h'}{\partial x} - \frac{2\delta^2}{æ^2}(\chi - 1)g\frac{h_o^3}{\nu^2}\frac{\partial}{\partial t}\left(h'\frac{\partial h'}{\partial t}\right)$$
$$+ \frac{\delta}{æ}\frac{\sigma h_o^3}{\rho\nu}\frac{\partial^4 h'}{\partial x^4} = 0 \quad (26)$$

where

$$c_o = 3q_o/h_o,\ c_1 = q_o(\chi + \sqrt{\chi^2 - \chi})/h_o$$
$$c_2 = q_o(\chi - \sqrt{\chi^2 - \chi})/h_o$$

Equation 26 has a typical two-wave structure. It means that the wave process on a liquid film includes a lower-order wave, whose velocity is c_o, and the waves described by the higher-order derivatives that propagate at velocities c_1 and c_2. The technique for deriving and analyzing such equations is discussed in detail by Whitham (1974).

Equation 26 may be successfully used as a basis in analyzing the falling film stability and the process of nonlinear wave formation.

In further considerations, the parabolic velocity profile $f(\eta) = (2\eta - \eta^2)$ in a gravitational vertical falling liquid film will be used. Therefrom the following coefficients will be calculated:

$$\delta = 2/3,\ æ = 2,\ \chi = 1{,}2,\ c_1 = 1.69u_o,$$
$$c_2 = 0.71u_o,\ u_o = q_o/h_o = gh_o^3/(3\nu)$$

After having substituted these coefficients into Eq. 26, we obtain in the dimensionless form

$$\left(\frac{\partial}{\partial\tilde{t}} + 3\frac{\partial}{\partial\tilde{x}}\right)H + 6H\frac{\partial H}{\partial\tilde{x}} - \frac{2}{15}Re\frac{\partial}{\partial\tilde{t}}\left(H\frac{\partial H}{\partial\tilde{t}}\right)$$
$$+ \frac{Re}{3}\left(\frac{\partial}{\partial\tilde{t}} + 1.69\frac{\partial}{\partial\tilde{x}}\right)\left(\frac{\partial}{\partial\tilde{t}} + 0.71\frac{\partial}{\partial\tilde{x}}\right)H + We\frac{\partial^4 H}{\partial\tilde{x}^4} = 0 \quad (27)$$

Here $H = h'/h_o$, $\tilde{x} = x/h_o$, $\tilde{t} = tU_o/h_o$, and $We = \sigma/\rho g h_o^2$ is the Weber number. Now let the obtained equation be analyzed.

a) Stationary Waves. Assuming that $h' = h'(x - ct)$, we integrate Eq. 27 over x:

$$(3 - \tilde{c})H + 3H^2 + \frac{Re}{3}\left(\tilde{c}^2 - 2.4\tilde{c} + 1.2 - \frac{2}{5}\tilde{c}^2\right)\frac{\partial H}{\partial\tilde{x}}$$
$$+ We\frac{\partial^3 H}{\partial\tilde{x}^3} = 0 \quad (28)$$

The dimensionless phase velocity $\tilde{c} = c/U_o$. Equation 28 completely coincides with the Shkadov (1967) equation, apart from the

capillary term nonlinearity which has been neglected from the very beginning.

b) Let $Re \sim 1$. As is seen from Eq. 27, it is the kinematic wave described by the equation

$$\frac{\partial H}{\partial \tilde{t}} + 3\frac{\partial H}{\partial \tilde{x}} = 0$$

that underlies the wave process. According to Whitham (1974), let the term $\partial/\partial\tilde{t}$ in the higher-order derivatives be substituted by $-3\partial/\partial\tilde{x}$ and the second nonlinear term be neglected. As a result, we obtain

$$\frac{\partial H}{\partial \tilde{t}} + 3\frac{\partial H}{\partial \tilde{x}} + 6H\frac{\partial H}{\partial \tilde{x}} + Re\frac{\partial^2 H}{\partial \tilde{x}^2} + W\frac{\partial^4 H}{\partial \tilde{x}^4} = 0 \quad (29)$$

This type of equation (however, with the coefficient 1.2 Re before the second derivative) has been used recently by Gjevik (1970), Maurin et al. (1977), Nepomnyashchii (1974), and Petviashvili and Tzvelodub (1978) as the basic equation for the analysis of nonlinear waves on vertical falling films.

c) $Re \gg 1$. The second-order waves are the basis of the wave process. Separate the wave that preliminarily propagates along the flow and can be described by the equation $\partial H/\partial\tilde{t} + 1.69\partial H/\partial\tilde{x} = 0$. In all the other derivatives of Eq. 27, let $\partial/\partial\tilde{t}$ be substituted by $-1.69\partial/\partial\tilde{x}$. Having integrated it over x, we obtain

$$\frac{\partial H}{\partial \tilde{t}} + 1.69\frac{\partial H}{\partial \tilde{x}} + 2.07H\frac{\partial H}{\partial \tilde{x}} - 4.01\frac{H}{Re} - \frac{9.2}{Re}H^2 - 3.06\frac{We}{Re}\frac{\partial^3 H}{\partial \tilde{x}^3} = 0 \quad (30)$$

This equation was obtained by Nakoryakov and Shreiber (1973) as a model to describe film surface waves at high Re numbers.

Thus in the case of a long-wave process at low Re numbers, the energy transfer from the mean flow to the kinematic wave follows the higher-order wave mechanism. This corresponds to the appearance of the energy source term (or "negative" viscosity term) in Eq. 29, beginning with the second derivative.

At high Re numbers the energy is transferred into a higher-order wave (which can conditionally be referred to as "inertial") by the kinematic wave. This corresponds to the appearance of the "low-frequency" energy source linear term in Eq. 30.

The film surface waves within a wide range of Re numbers should be analyzed on the basis of Eq. 27. The conclusions concerning the exact range of its applicability and the possibility of the transition, in Eq. 27, to the case of very high Re numbers can be drawn only from the comparison between its solutions and the experimental results. Such a comparison for the case of linear waves is given in the later section on two-dimensional waves in the inception region.

LINEAR ANALYSIS OF FILM FLOW STABILITY

Let the dispersion equations for temporally growing (damped) waves be derived. With this end in view, let H be represented as

$$H \sim \exp[i(k\tilde{x} - \Omega\tilde{t})] = \exp[i(k\tilde{x} - \omega\tilde{t})] \cdot \exp\beta\tilde{t} = \exp[ik(\tilde{x} - \tilde{c}\tilde{t})]\exp\beta\tilde{t}$$

where $k = 2\pi h_o/\lambda$ is the real wave number, $\Omega = \omega + i\beta$ the complex frequency which is made dimensionless by using h_o and U_o, and $\tilde{c} = c/u_o$ the real part of the phase velocity. After having substituted H into the linearized Eq. 27 and having separated the real and the imaginary parts, we arrive at

$$-\tilde{c} + 3 - \frac{2}{3}\tilde{c}\beta Re + 0.8Re\beta = 0 \quad (31)$$

$$3\beta - k^2Re(\tilde{c}^2 - 2.4\tilde{c} + 1.2) + Re\beta^2 + 3We \cdot k^4 = 0 \quad (32)$$

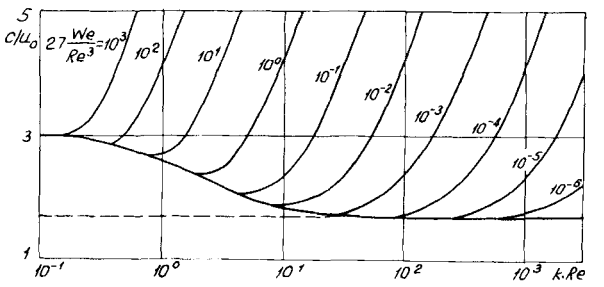

Figure 2. Dispersion curves for two-dimensional waves on a vertical falling liquid film.

Similar equations were derived by Shkadov (1968) directly from the system of Eqs. 15 and 16, however the dispersion relations were not analyzed.

It follows from Eq. 31 that

$$\beta Re = -\frac{3}{2}\frac{\tilde{c} - 3}{\tilde{c} - 1.2} \quad (33)$$

Excluding β from Eq. 32, let the quadratic (with respect to k^2Re^2) equation

$$(kRe)^4 - (kRe)^2\frac{Re^3}{3We}(\tilde{c} - \tilde{c}_1)(\tilde{c} - \tilde{c}_2) - \frac{3Re^3(\tilde{c} - 3)(\tilde{c} + 0.6)}{4We(\tilde{c} - 1.2)^2} = 0$$

where $\tilde{c}_1 = 1.69$, $\tilde{c}_2 = 0.71$, be derived by means of Eq. 33.

Its solution is

$$(kRe)^2 = \frac{Re^3}{6We}(\tilde{c} - \tilde{c}_1)(\tilde{c} - \tilde{c}_2) \times \left[1 \pm \sqrt{1 + \frac{27We(\tilde{c} - 3)(\tilde{c} + 0.6)}{Re^3(\tilde{c} - 1.2)^2(\tilde{c} - \tilde{c}_1)^2(\tilde{c} - \tilde{c}_2)^2}}\right] \quad (34)$$

Equation 34 has two pairs of roots, to which correspond the two nonintersecting branches of the dispersion curve, symmetrical to each other relative to the axis $\tilde{c} = 1.2$. All the above-mentioned also refers to the growth rates, whose axis of symmetry is the line $\beta = -1.5/Re$. Later on we will consider solely the upper branches of the dispersion curves given in Figure 2. The appropriate values of the growth rates are given in Figure 3.

It follows from Eqs. 32–33 that neutral waves ($\beta = 0$) exist under the conditions

$$\tilde{c} = 3,\ k_1 = \sqrt{Re/We},\ k_2 = 0 \quad (35)$$

Waves with $\tilde{c} > 3$ are exponentially damped, while those with

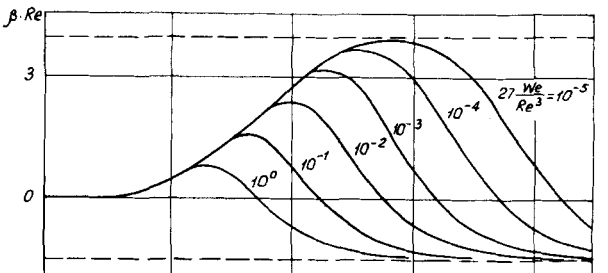

Figure 3. Temporal growth rate of a film.

$\tilde{c} < 3$ grow. The asymptotics of the dispersion curves in the region $\tilde{c} > 3$ is obtained from Eq. 34, provided that the righthand term in the radicand is neglected:

$$\tilde{c} = 1.2 + \frac{\sqrt{6}}{5}\sqrt{1 + \frac{25}{2}\frac{We}{Re}k^2}$$

For $Re \sim 1$ and not very low k (which corresponds to capillary ripples in front of large waves propagating over the thin residual layer), we have

$$\tilde{c} = 1.2 + k\sqrt{3We/Re} \tag{36}$$

In the coordinate system moving at the velocity $1.2\ U_o$, expression 36 exactly coincides with the dispersion formula for capillary waves on shallow water.

The analysis of Eq. 33 shows that the maximum growth rate corresponds to the minimum phase velocity. Hence, the fastest growing waves line will intersect the dispersion curves in Figure 2 at the points of the minimum phase velocities. To accurately determine the characteristics of the fastest growing waves, come back to Eqs. 32–33.

We rewrite Eq. 33 as

$$\tilde{c} = 1.2 + 1.8/\phi \tag{37}$$

where

$$\phi = 1 + \frac{2}{3}Re\beta \geq 1$$

After having substituted Eq. 37 into Eq. 32, we differentiate the expression with respect to k and allowing for the extremum condition $\partial\phi/\partial k = 0$, we obtain

$$kRe = 0.2\sqrt{\frac{Re^3}{We}}\sqrt{\frac{13.5}{\phi^2} - 1} = \sqrt[4]{\frac{3}{4}\frac{Re^3}{We}(\phi^2 - 1)} \tag{38}$$

Finally, after having substituted Eqs. 37 and 38 into Eq. 32, we arrive at

$$\frac{Re^3}{We} = \frac{\phi^4(\phi^2 - 1)}{(\phi^2 - 13.5)^2}\frac{3.10^3}{6.4} \tag{39}$$

The maximum growth rate is

$$\beta = \frac{3}{2}(\phi - 1)/Re \tag{40}$$

To pass from the temporal growth rate β to the spatial growth rate $(-\alpha)$ (these are the rates that are measured in the experiments), the known Gaster transformation

$$-\alpha = \beta \Big/ \frac{\partial\omega}{\partial k} = \beta \Big/ \left[\tilde{c} + k\frac{\partial\tilde{c}}{\partial k}\right] = \beta/\tilde{c} \tag{41}$$

should be used. Here we have taken into account that for the fastest growing waves $\partial\tilde{c}/\partial k = 0$. The numerical calculation shows that within the framework of the problem formulated, the temporal and the spatial growth rates are related by Eq. 41 with a sufficient accuracy.

Thus the system of formulae in Eqs. 37–41 describes all the characteristics of the fastest growing waves in the parametric form.

Since Re and We enter the dispersion equation as the ratio Re^3/We, it should be transformed so that only one flow rate parameter, Re, is used:

$$\frac{Re^3}{We} = 3^{2/3}(Re/Fi^{1/11})^{11/3}$$

EXPERIMENTAL PROCEDURE

The experiments dealing with the waves in the inception region were performed on a setup described by Pokusaev and Alekseenko (1977). Liquid from a constant-level tank flowed through a liquid distributor onto the outer surface of a test section, which was a 1 m long, 60 mm dia. Plexiglass tube. Due to the experimental requirements, while measuring the instantaneous velocity profile we used a stainless steel tube of 60.8 mm dia and high-polished (mirror) surface.

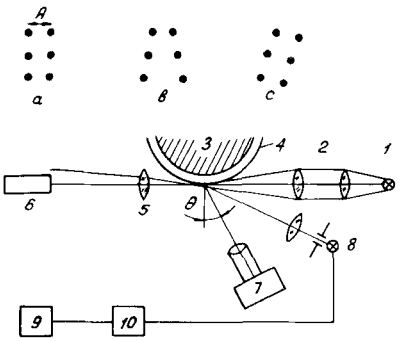

Figure 4. Scheme of the film thickness and velocity profile measurements.

Liquid flowed to the test section through a 70 mm long and 0.5–1 mm wide annular orifice. While preparing the experiment, the main difficulty was to insure the two-dimensional flow of the wave liquid film. To be uniformly wetted, the test section was made strictly vertical and the annular gap and the coaxility between the liquid distributor and the test section were fine-adjusted until two-dimensional (annular) waves were obtained. This adjustment was possible due to the small clearance between the setting surfaces of the test section and the liquid distributor.

Liquid films are extremely sensitive to external disturbances, e.g., to vibrations induced by an operating pump. Therefore, the experiments were performed only with the pump switched off, and the liquid was pumped into the upper tank periodically in an automatic way.

As a working liquid we used aqueous glycerine solutions, since they are less affected by surfactants absorbing on the liquid film as compared to pure water. In addition, as follows from our observations, two-dimensional waves on a water-glycerine film appear to be more stable to three-dimensional disturbances and remain for sufficiently great path lengths.

Experimentally measured variables were: instantaneous and mean thickness of the film, wave amplitudes, velocities and lengths, as well as instantaneous velocity profiles in a wave flow regime.

The film thickness was measured by a shadow method shown in Figure 4. The gist of the method is as follows. Power light source *1* (mercury lamp) via condenser *2* tangentially irradiates test section *3*, and liquid film *4* falling over the outer surface of the vertical tube forms a shadow. Magnified film shadow pulsations are projected by objective lens *5* to photoelectron multiplier *6* and recorded in analog or digital form.

The phase velocity of the waves was measured by the phase shift between two simultaneous recordings of the instantaneous film thickness which corresponded to two different points along the tube.

The accuracy of the absolute thickness and phase velocity measurements is 2–5 and 5–9%, respectively.

The instantaneous velocity field in a wave liquid film was estimated by two synchronized methods: the shadow method for thickness determination, and by stroboscopic particle visualization, by means of which velocities could be measured. The latter was first used in a similar way by Cook and Clark (1971) and Ganchev et al. (1972), who measured the mean velocity profile only. The process of measuring the instantaneous velocity profile in a wave liquid film is schematically shown in Figure 4. Liquid film *4* with small concentrations of 1–5 μ round aluminium particles falls over the outer surface of stainless steel, high-polished tube *3*. If the particles are recorded by camera *7* with lateral pulse irradiation by lamp *8*, then the film frame fixes a discontinuous track of one particle from which, provided that the frequency and the magnification factor are known, the particle velocity can be determined. The pulse frequency of lamp *8* is set by sonic frequency generator *9* triggering stroboscope *10*.

With the mirror surface of the test section being high-polished, in taking photographs at an angle θ to the normal relative to the surface the camera will record not only the track of a real particle, but also that of a particle virtual image, formed by the mirror, as illustrated by details a–c in Figure 4. By simple geometric constructions, the formula

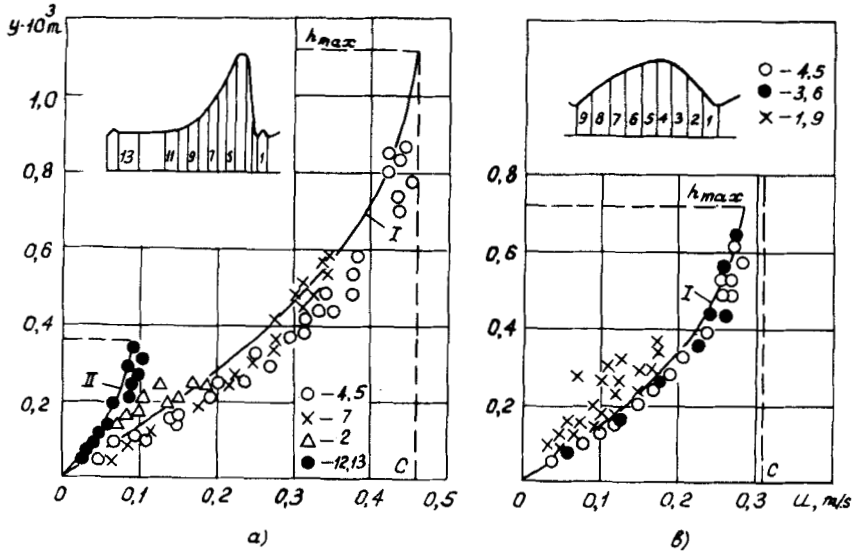

Figure 5. Instantaneous velocity profiles in a wave liquid film.

Wave characteristics as in Table 1; curve derivation explained in text.

TABLE 1. WAVE CHARACTERISTICS, FIGURE 5.

Fig.	$\nu\cdot10^6$ m^2/s	$\langle h\rangle$ mm	h_{max} mm	λ mm	C mm/s	$C\ q_o/\langle h\rangle$	$\frac{\langle U\rangle}{q_o/\langle h\rangle}$
5a	7.2	0.545	1.12	36	460	2.83	1.27
5b	7.1	0.56	0.73	11.8	310	1.93	1.48

$$y = \frac{A}{2N\sin\theta}\sqrt{n^2 + tg^2\theta(n^2-1)} \tag{42}$$

is derived, where N is the magnification factor measured without liquid in a plane parallel to the film frame, n the liquid refraction, and A the distance between the real and the virtual images of the particle on the photographic film.

Figure 4a–c, illustrates typical double tracks of particles, when the number of pulses is equal to three. Case (a) corresponds to the smooth film, in the presence of a longitudinal velocity component only, calculated by the formula

$$u = (x_{i+1} - x_i)/(N_f) \tag{43}$$

where x_i is the longitudinal coordinate of the particle image on the film at the ith pulse, f being the pulse frequency. Case (b) corresponds to the smooth film, but the transverse velocity component also is available; it is equal to

$$v = (y_{i+1} - y_i)f \tag{44}$$

where y_i is the transverse particle coordinate calculated by formula 42. Case (c) corresponds to the wave liquid film when the surface is inclined at a certain angle to the longitudinal axis x.

The analysis of the profiles of the two-dimensional waves observed in the experiments with low Re numbers, shows that this angle reaches its maximum value (23°) only in the region of the leading front of the largest

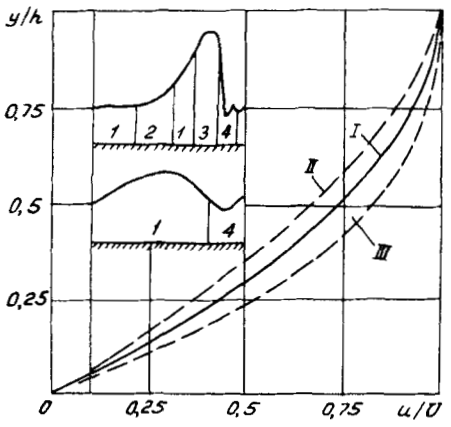

Figure 6. Dimensionless velocity profile.

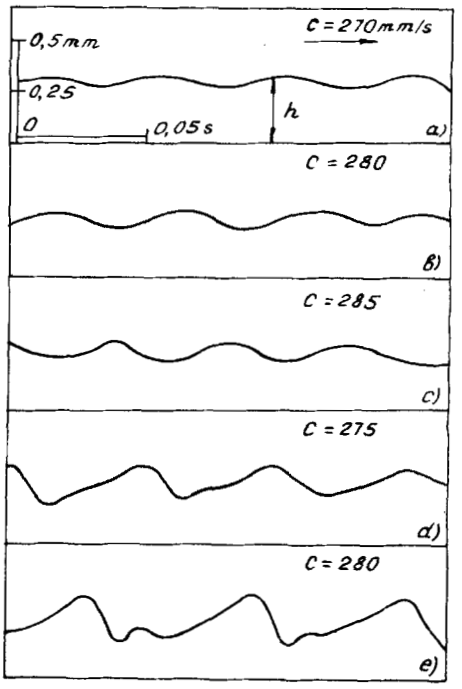

Figure 7. Wave evolution on a vertical falling liquid film.

$\nu = 2.34\cdot10^{-6}$ m²/s; $\sigma/\rho = 60.2\cdot10^{-6}$ m³/s²; $Re = 15.3$; x/h_o = (a) 155, (b) 165, (c) 185, (d) 200, (e) 240.

waves. In this case, an additional error in determining y and U amounts to 3 and 6.5%, respectively, for the case when $\theta = 30°$. For small and large waves (except for their leading front), formulae 42–44 can be used. The main experimental errors are: 7% for the absolute values of y, 2% for its relative values, and 4–5% for the longitudinal velocity.

The position of a particle in a wave was determined by simultaneously recording the thickness of the film and the moments of the lamp pulses.

As a rule, a photographic film frame contained 5–10 tracks responsible for a small part of the film. The velocity field over the total wavelength was constructed on the basis of 30–50 frames. It is very important in this case that the waves be strict-regular and two-dimensional, since the velocity distribution is estimated by a set of data for various waves.

INSTANTANEOUS VELOCITY PROFILE IN A WAVE LIQUID FILM

Despite the fact that ample data concerning liquid velocities in a film are known, the results of measuring the instantaneous velocity profile in a wave liquid film are absent from the literature, although these data are considered to be of special interest in formulating the theory.

As has been mentioned above, the method of velocity measurements requires strict-regular periodic waves. For this purpose, artificial disturbances were superimposed on the film flow by means of liquid flow rate pulsations, as carried out by Kapitza and Kapitza (1949) and Pokusaev and Alekseenko (1977). As a result, strict-regular two-dimensional stationary periodic waves were formed. The picture of the stationary excited waves at a given Re is determined only by the frequency of the superimposed disturbances. If the frequencies of the natural stationary waves and those of the superimposed disturbances coincide, the wave pictures are identical, i.e., the natural wave regime is a particular case of the stationary excited waves.

The results of measuring the instantaneous longitudinal velocity profiles for the characteristic value of $Re = 12.4$ and the two characteristic types of the observed waves are given in Figure 5. Above each wave profile the sections are shown for which the velocity profiles have been constructed. The points correspond to the section numbers. Curve I is the self-similar parabolic profile plotted according to the maximum thickness and velocity values. Curve II is the Nusselt velocity profile for a smooth laminar film, plotted according to the residual layer thickness. The dotted line designates the wave phase velocity. The other characteristics of the wave regimes are listed in Table 1.

The above plots show that in the region of the maximum film thicknesses the velocity profile changes insignificantly, while at the minimum values of h (sections *1* and *9*, Figure 5b, and section *2*, Figure 5a), it undergoes great changes. In the residual layer region the flow is purely laminar and can be described by the Nusselt theory (curve II in Figure 5a). The maximum liquid velocities in a wave reach the values of the wave phase velocities (Figure 5a).

The analysis of the results shows that for a given wave section, the greater values of the longitudinal velocity correspond to the higher values of the y coordinate. This points to the absence of a stationary vortex even for the waves of so large an amplitude as shown in Figure 5a.

The results of the velocity profile measurements are schematically shown in Figure 6 in the dimensionless coordinates $[y/h; u/U]$, where h is the local thickness, U the local surface velocity calculated according to the velocity of particles-marks detected near the film surface (curve I is a self-similar parabolic profile). The wave profiles here are roughly divided into sections. In section *1* the velocity profile is described by the self-similar parabolic law. In section *2* the velocity profile is less filled as compared to the parabolic one, and corresponds to region II, while in section 3 it is more filled (region III). The maximum deviations from the parabolic law amount to 15%. For section *4*, no velocity profile has been plotted due to great scattering of the experimental points.

TWO-DIMENSIONAL WAVES IN THE INCEPTION REGION

A vertical falling liquid film at $Re = 5 \rightarrow 50$ can be described as follows. In close proximity to the outlet orifice the liquid film is smooth. Then, at a certain distance from the orifice edge, due to the natural instability of the smooth laminar flow, infinitesimal two-dimensional periodic disturbances arise, their amplitude growing fast. At sufficiently large amplitudes, nonlinearity can be observed and the wave regime becomes stationary and nonlinear. The two-dimensional waves are unsteady and soon break into

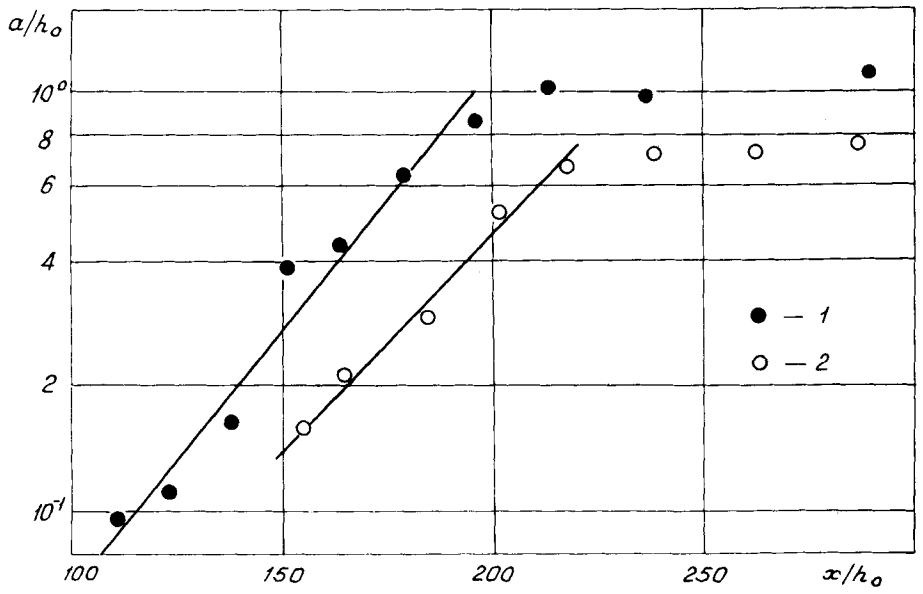

Figure 8. Amplitude of growing waves.

$\nu = 2.34 \cdot 10^{-6}$ m²/s; $\sigma/\rho = 60.2 \cdot 10^{-6}$ m³/s²; Re = (1) 36.4, (2) 15.3.

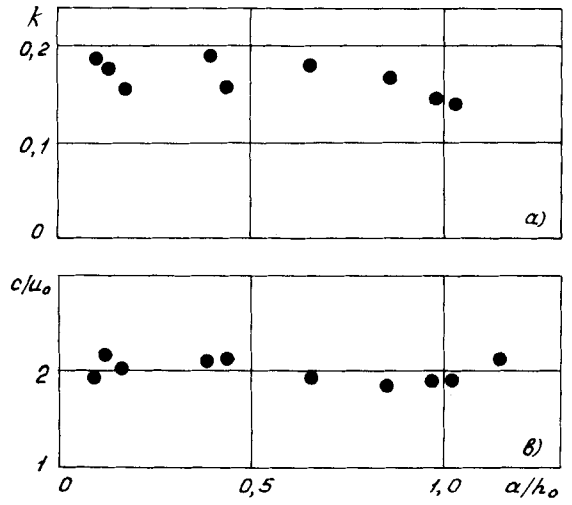

Figure 9. Wave number (a) and phase velocity (b) of growing waves.

$\nu = 2.34 \cdot 10^{-6}$ m²/s; $\sigma/\rho = 60.2 \cdot 10^{-6}$ m³/s².

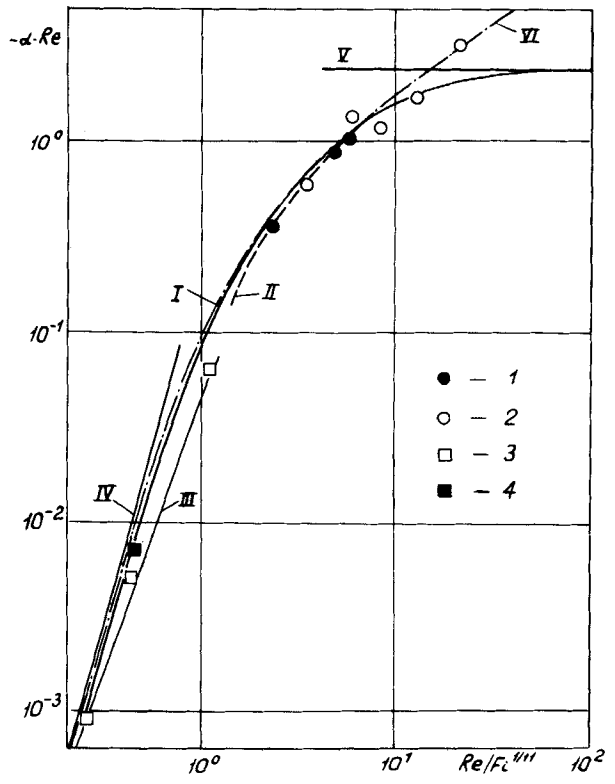

Figure 10. Spatial growth rates.

Experimental data:
1. ● $\nu = 2.34 \cdot 10^{-6}$ m²/s; $\sigma/\rho = 60.2\ 10^{-6}$·m³/s².
2. ○ Portalski and Clegg (1972); $Fi^{1/11} \approx 5.33$.
3. □ Krantz and Goren (1971), oil; $Fi^{1/11} \approx 1.19$.
4. ■ Krantz and Goren (1971), oil; $Fi^{1/11} \approx 1.72$.

Theoretical data (curves):
I Present study, Eqs. 39–41.
II Whitaker (1964), water.
III Benjamin (1957).
IV Long-wave approximation, Benjamin (1957).
V Nakoryakov and Schreiber (1973), linearized Eq. 30.
VI Pierson and Whitaker (1977).

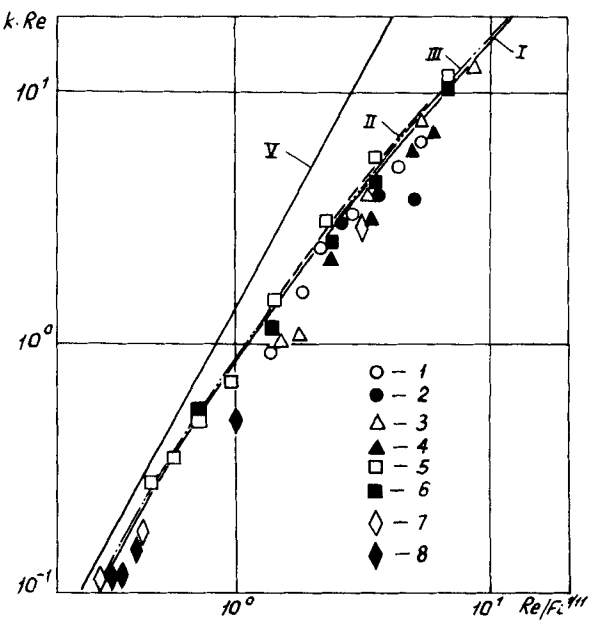

Figure 11. Wave number of growing waves.

Experimental data (symbols): see Table 3.
Theories of the fastest growing waves (curves):
I Present study, Eqs. 38 and 39.
II Whitaker (1964), water.
III Pierson and Whitaker (1977), water; $Fi^{1/11} = 9.2$.
[IV omitted]
V Neutral curve, present study, Eq. 35.

three-dimensional disturbances which are essentially nonstationary.

Data concerning the evolution of the two-dimensional waves in their inception region are given in Figures 7–9. The film thickness oscillograms were taken at various distances from the outlet orifice edge, by moving the optical system along the test section. As follows from Figures 7 and 8, the arising waves are sinusoidal and their amplitude ($a = h_{max} - h_{min}$) first grows exponentially with distance and then becomes constant. For the sake of convenience, the velocity and wavelength data are given in Figure 9 as a function of the amplitude, whence directly follows the linearity of the waves in the inception region.

It should be noted that the arising waves are not strict-regular; therefore, to obtain average wave characteristics the signal should be statistically analyzed. However, with the properly organized supply of the liquid to the test region and suitable properties and flow rates of the liquid, fairly regular two-dimensional waves could be observed in the inception region. Where possible, we considered just these regimes.

According to the linear theories of wave instability, the waves actually observed near the wave inception line should correspond to the fastest growing waves, which has been partially confirmed in several publications. Thus Pierson and Whitaker (1977) and others reported on the experimental data for wavelengths and velocities of water films alone, Krantz and Goren (1971) performed measurements at $Re \lesssim 1$ for oil films only. Figures 10–12 generalize our and other authors' experimental results on the growth rates, the velocities, and the lengths of the growing waves, and compare them with the linear theories of the fastest growing waves. While plotting, the coordinates were chosen so that our theoretical dependencies would be universal curves.

The growth rate was estimated according to the tangent of the inclination angle of the lines in Figure 8, the angle having been plotted in the semilog coordinates:

TABLE 2. ASYMPTOTIC VALUES OF FASTEST GROWING WAVES AT LIMITING Re VALUES WITH Fi = CONST.

	$Re \to 0$		$Re \to \infty$	
	Anshus	Present Study	Anshus	Present Study
$-\alpha \cdot Re$	Const $Re^{11/3}$	Const $Re^{11/3}$	Const $Re^{2/3}$	Const
$k \cdot Re$	Const $Re^{11/6}$	Const $Re^{11/6}$	Const $Re^{4/3}$	Const $Re^{11/12}$
c/U_o	Const = 3	Const = 3	Const = 1.5	Const = 1.69

$$-\alpha = \left[\ln \frac{a_1 - a_2}{h_o}\right] \Big/ \left(\frac{x_1 - x_2}{h_o}\right)$$

The approximating lines were obtained by the least squares method.

In the region of $Re > 10$, our experimental data for a water-glycerine solution are in agreement with those obtained by Portalski and Clegg (1972). At $Re \lesssim 1$, Krantz and Goren's data (1971) for oil films are given.

At $Re/Fi^{1/11} < 0.5$, the experimental points can be well described by various theories, as listed in the curve identifications in Figure 10. It should be noted that in the original study by Benjamin (1957), the growth rate in formulae 5–10 is erroneous (later he corrected the mistake), i.e. 0.224 should be substituted by 0.448. In the range of moderate Re numbers, at $Re/Fi^{1/11} > 2$, the experimental data can be well generalized by theoretical relations I and VI and partially by II.

In Figures 11 and 12, the neutral curves for the wave number and the velocity are also presented; however, they significantly deviate from the experimental points. The experimental velocities are considerably scattered, which is due to the difficulty of measuring the wave characteristics for small-amplitude waves of very smooth slope form. However, reasonable agreement between the experiment and the fastest growing waves theories can be observed.

The plots given in Figures 7–12 show that in the wave inception region, the behavior of the growing waves at the initial stage of their evolution can be described by the linear theories of the fastest growing waves. Curve I in Figures 10–12, despite the simplicity of the equations used for the derivation, fairly well generalizes the experimental points and is in agreement with the other theories in a wide range of $Re/Fi^{1/11}$ variations, which is one of the proofs concerning the versatility of two-wave Eq. 27.

Letting the results of the numerical calculation according to the Orr-Sommerfeld equation in Pierson and Whitaker's study (1977) be valid in a given range of Re numbers, a more accurate conclusion on the applicability field of the boundary layer approximation for a liquid film can be made from the comparison of curves I and VI in Figure 10. As is seen therefrom, the best agreement between I and VI can be observed in the range of $1 \leq Re/Fi^{1/11} \leq 10$. However, at $Re/Fi^{1/11} < 1$, the correlation between the theories can also be considered as fairly reasonable, since the dependencies differ in the constant numerical coefficient only, but have the same asymptotics with respect to Re. A more significant discrepancy can be observed at $Re/Fi^{1/11} > 10$, since the theoretical dependencies have different asymptotics. Anshus (1972) considered the asymptotic solutions of the Orr-Sommerfeld equation at $Re \to \infty$, and they are in agreement with the calculations made by Pierson and Whitaker (1977). For comparison, in Table 2 we present the asymptotic values of the fastest growing waves characteristics for two limiting cases of low and high Re numbers, at Fi = const.

NONLINEAR STATIONARY WAVES

As has been mentioned above, the evolution of the developing waves results in a finite-amplitude stationary regime. However, to experimentally investigate the two-dimensional stationary waves turns out to be very difficult, since the two-dimensional waves trend toward breaking due to their instability to the three-dimensional disturbances. Besides, owing to some stochasticity of the wave formation process, strict-regular waves cannot be observed.

To thoroughly investigate precisely the two-dimensional stationary waves, artificial disturbances (i.e., periodic flow rate fluctuations) were superimposed on the main flow. In so doing, within the range of Re numbers $\lesssim 70$, at distances up to 300–700 mm from the inlet, two-dimensional stationary waves existed, which will later be on referred to as excited waves. The most remarkable peculiarity of these waves is that at a sufficient level of flow rate fluctuations the picture of the steady-state waves is determined by the fluctuation frequency only, but does not depend on the amplitude, which means that the wave regime is one-parametric. The profiles of the excited waves, depending on the frequency of the superimposed fluctuations, are shown in Figure 13 for Re = 8.05. With high frequencies, the amplitude of the waves is small and their form is almost sinusoidal (Figure 13c). As fast as the frequency decreases, the phase velocity, the length, and the amplitude of the waves grow and their shape becomes asymmetric (Figure 13a,b). It has been experimentally shown that regime (a) may be considered as a sequence of stationary solitary waves traveling over a thin residual layer, its thickness being h_R.

It seems to be very important to lay emphasis on another experimental fact, i.e., that with the frequencies of the natural and of the excited waves coinciding, the observed wave pictures are identical. It means that the two-dimensional stationary natural waves are a particular case of the excited waves, when the frequency value is due to the conditions of the amplitude growth maximum velocity.

The excited waves exist within a limited frequency range f_{min}, $f_{min} < f < f_{max}$ (at a given Re). The region of their existence is roughly shown in Figure 14 in the coordinates $(k \cdot Re, Re/Fi^{1/11})$. Here the neutral curve and the dependence for the fastest growing waves are also given. With $f > f_{max}$, the excited waves have a very small amplitude and quickly lose their stability. As a result, a natural wave regime, similar to that without disturbances superposition, is realized. With $f < f_{min}$, the distance between the solitary waves is so great that new waves succeed in having developed on

TABLE 3. DATA FOR SYMBOLS, FIGURES 11 AND 12.

Symb. No.	Source	Fluid	$\nu \cdot 10^6$ m^2/s	$\sigma/\rho \cdot 10^6$ m^3/s^2	$Fi^{1/11}$	Re
1	Present study	Aqueous glycerin solution	2.12	65.3	6.78	10–40
2	Present study	Aqueous ethanol solution	2.12	28.5	5.42	10–27
3	Present study	Aqueous glycerin solution	3.72	61	5.46	8–48
4	Present study	Aqueous solution of ethanol and glycerin	2.34	60.2	6.4	15–36
5	Jones & Whitaker (1966)	Water	—	—	9.54	6.70
6	Strobel & Whitaker (1969)	Water	—	—	9.54	6.70
7	Krantz & Goren (1971)	Mineral oil	—	—	1.72	0.5–5.5
8	Krantz & Goren (1971)	Mineral oil			1.14	0.25–1.2

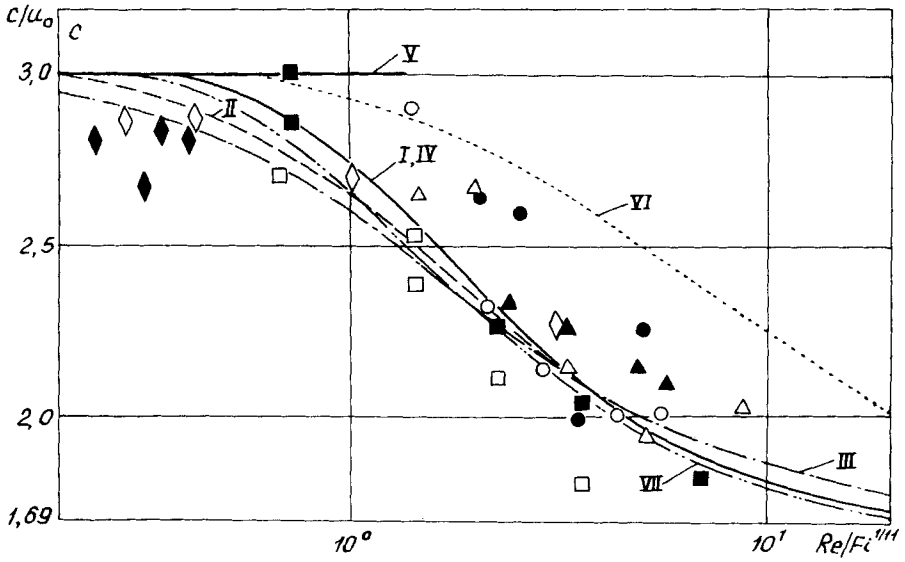

Figure 12. Phase velocity of growing waves.

Experimental data (symbols): see Fig. 11 for numbering code, see Table 3 for data.
Theories of the fastest growing waves (curves):
I Present study, Eqs. 37–39.
II Whitaker (1964), water.
III Krantz and Goren (1971), oil; $Fi^{1/11} = 1.72$.
IV Krantz and Goren (1971), water; $Fi^{1/11} = 1.72$.
Neutral curves:
V Present study, Eq. 35, and long-wave approximation, Benjamin (1957).
VI Krylov et al. (1969), water.

the residual layer due to the natural instability, and the regular wave picture is destroyed.

The characteristics of the stationary waves in the dimensionless coordinates are given in Figures 15–16. The independent wave parameter is the wave number k. However, the amplitude of the waves is presented as a function of the phase velocity to demonstrate the rigorous linear relationship between these values.

It should also be noted that although all the nonlinear theories predict the decrease of the mean film thickness in the wave regime, this fact, obviously, has been experimentally corroborated in the present paper alone (Figure 16).

The excited-wave theories appear to be a convenient object to compare with the stationary-wave theories, since it does not seem necessary in this case to involve any hypotheses (typically invalid) concerning the choice of one solution between a set of probable theoretical solutions. Examples of the wave profiles, calculated by Tzvelodub (1980) according to Eq. 29 (however, with the coefficient 1.2 Re before the second derivative) are given in Figure 17. Similar results have also been obtained for Eq. 28. The limit of periodic waves for $k \to 0$ is a soliton solution (Figure 17d). Comparison of Figures 13 and 17 shows that the theory and the experiment are here in qualitative agreement.

EVOLUTION OF INITIAL STATIONARY DISTURBANCES

To use Eq. 27 and analyze the wave formation mechanism to the full, one can study the evolution of the initial solitary disturbances of the film thickness. With this end in view, we specified such a liquid flow rate during the experiments so that the flow

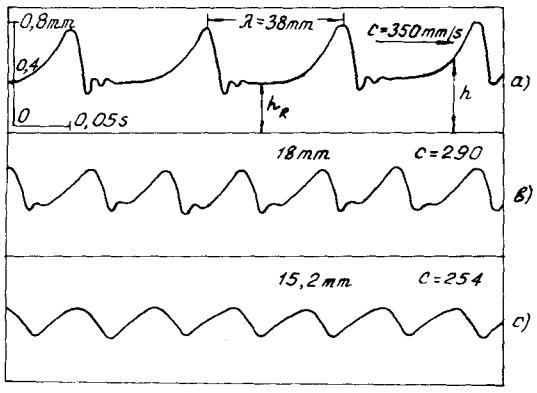

Figure 13. Profiles of stationary excited waves.

$Re = 8.05$; $\nu = 7.2 \cdot 10^{-6}$ m²/s; $\sigma/\rho = 57.6 \cdot 10^{-6}$ m³/s².

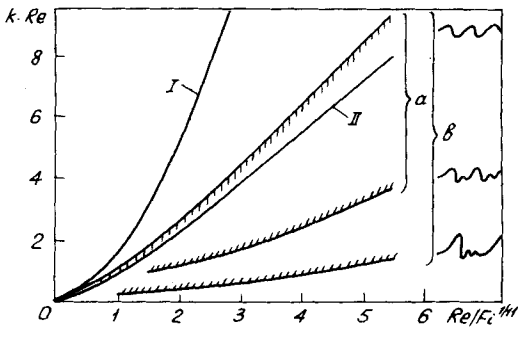

Figure 14. Existence regions of (a) natural, and (b) disturbed stationary waves.

I Neutral curve, Eq. 35,
II Line of the fastest growing waves, Eq. 38.

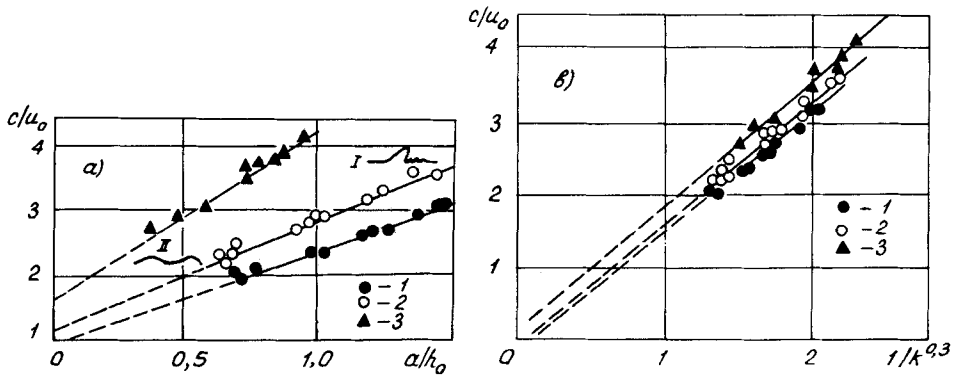

Figure 15. Dependencies of stationary periodic waves velocity on (a) amplitude, and (b) wave number.

$\nu = 11.2 \cdot 10^{-6}$ m²/s; $\sigma/\rho = 55.9 \cdot 10^{-6}$ m³/s²; Re = 12.4(1), 7.85(2), 4.0(3).

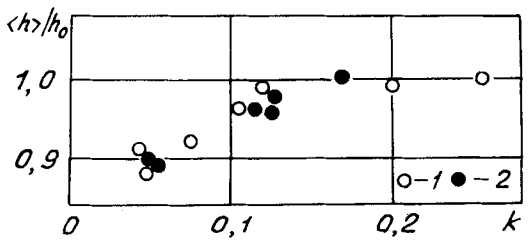

Figure 16. Influence of waves on average thickness of a film.

$\nu = 2.06 \cdot 10^{-6}$ m³/s; $\sigma/\rho = 40.3 \cdot 10^{-6}$ m³/s²; Re = 30.3(1), 20.4(2).

would be smooth ($Re < Re_*$ = 3–5, where Re_* is the conditional critical wave formation Re number estimated visually in our experiments). Then a standard flow rate pulse was generated which could be adjusted according to amplitude, length, and form. The evolution of the thickness disturbances developes thereby was followed by way of recording the film thickness at various distances from the inlet. Some experimental results are given in Figures 18–21.

In Figure 18 the evolution of the "stepwise" disturbances generated by way of sudden increase (positive steps) or decrease (negative steps) in the flow rate, are given. Two values of Re number are specified, i.e., $Re = gh_o^3/3\nu^2$, the Reynolds number of the layer over which the disturbance is spread; and $Re^* = gh^{*3}/3\nu^2$, the Reynolds number of the layer beyond the step front.

The stationary steps are always formed from positive pulses. Thereby, at $Re^* < Re_*$ the steps are smooth. At $Re^* \to Re_*$ weak fluctuations can be observed to the right and to the left of the step front. At $Re^* > Re_*$ a developed wave regime appears beyond the step front.

The formation of the stationary smooth step seems evidently to take place due to the concurrence of the front nonlinear steepening, as well as to the dissipative diffusion owing to the surface tension. The negative semiinfinite disturbances are merely nonstationary, since both the nonlinearity and the surface tension result in one and the same effect, i.e., the diffusion of the front. The velocity of the

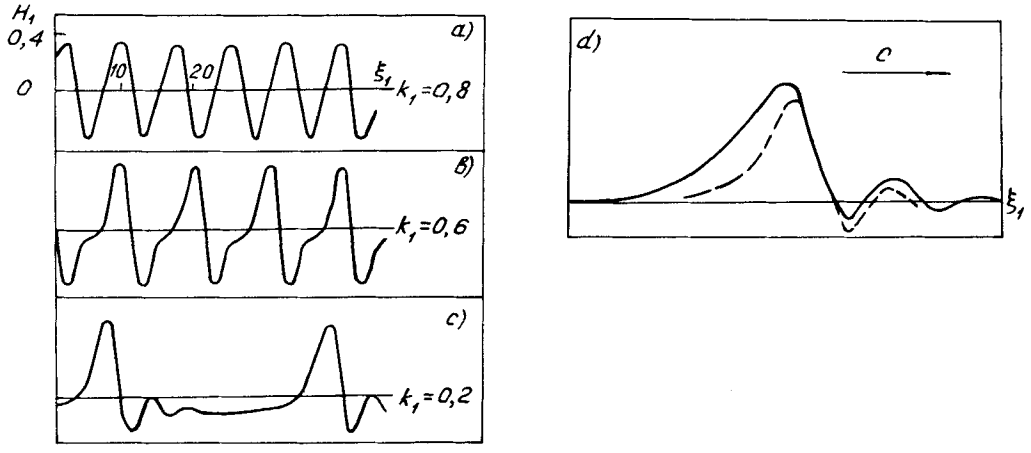

Fig. 17. Theoretical profiles of stationary waves, calculated by Tzvelodub (1980).

$$k_1 = k\left(\frac{We}{1{,}2Re}\right)^{1/2},\quad H_1 = (h - h_o)\Big/\left[0.8 \cdot Re\left(\frac{1{,}2Re}{We}\right)^{1/2}\right] h_o$$

$$\xi_1 = (1{,}2Re/We)^{1/2} \cdot x/h_o$$

(d) Soliton solution; - - - theoretical profile.

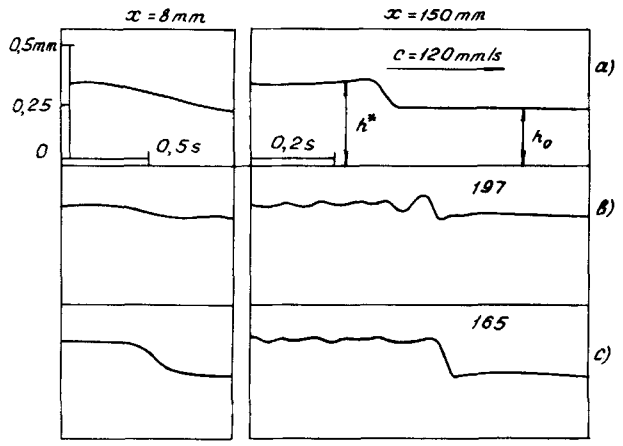

Figure 18. Evolution of positive steps.

(a) $\nu = 7.8 \cdot 10^{-6}$ m²/s; $\sigma/\rho = 56.7 \cdot 10^{-6}$ m³/s²; $Re = 0.67$; $Re^* = 2.35$.
(b) $Re = 2.35$; $Re^* = 3.66$.
(c) $Re = 1.02$; $Re^* = 3.85$.

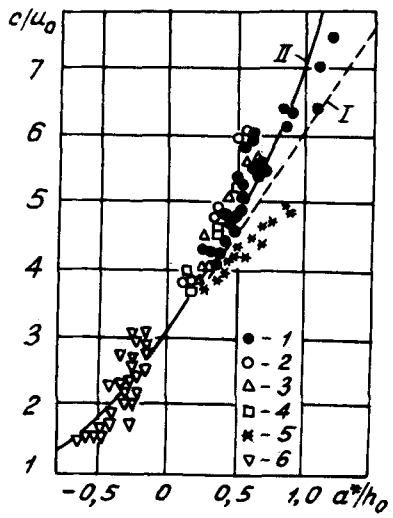

Figure 19. Velocity of solitary disturbances.

1. ● Positive steps; $\nu = 8.05 \cdot 10^{-6}$ m²/s; $\sigma/\rho = 56.5 \cdot 10^{-6}$ m³/s²; $Re = 1.1$; $x = 25 \div 185$ mm.
2. ○ Positive steps; $\nu = 7.8 \cdot 10^{-6}$ m²/s; $\sigma/\rho = 56.7 \cdot 10^{-6}$ m³/s²; $Re = 0.74 \div 4.3$; $x = 150$ mm.
3. △ Triangular waves (Fig. 20a); $x > 60$ mm, other data as in (2) above.
4. □ Triangular waves; data as in (3) above.
5. * Positive localized disturbances (Fig. 20b); $x > 150$ mm; other data as in (2) above.
6. ▽ Negative disturbances (velocity of the trailing front; Fig. 21).

I Eq. 45.
II Eq. 46.

stationary step can be calculated according to Eq. 29, provided that we have passed to the wave-associated coordinate system and integrated the equation over x, from $+\infty$ to $-\infty$:

$$\frac{c}{u_o} = 3 + 3\frac{a^*}{h_o} \tag{45}$$

where $a^* = h^* - h_o$ is the amplitude of the wave.

A similar expression can also be obtained from Eq. 27. However, this calculation yields an underrated value of the velocity, as is seen from the comparison of the theory and the experiment (Figure 19). One can achieve better agreement, considering the flow rate balance of the wave

$$(c - u^*)h^* = (c - u_o)h_o$$

whence

$$\frac{c}{u_o} = 3 + 3\frac{a^*}{h_o} + \left(\frac{a^*}{h_o}\right)^2 \tag{46}$$

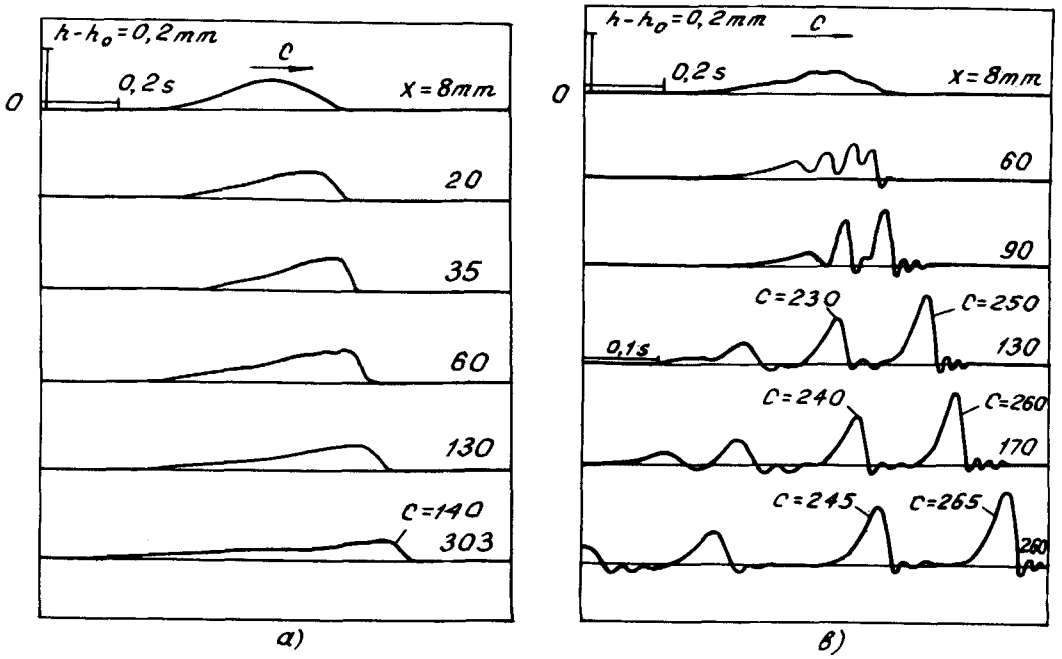

Figure 20. Evolution of an initial solitary disturbance.

$\nu = 7.5 \cdot 10^{-6}$ m²/s; $\sigma/\rho = 57 \cdot 10^{-6}$ m³/s².
(a) $h_o = 0.29$ mm; $Re = 1.5$; $Re^* = 3.5$.
(b) $h_o = 0.39$; $Re = 3.05$; $Re^* = 6$.

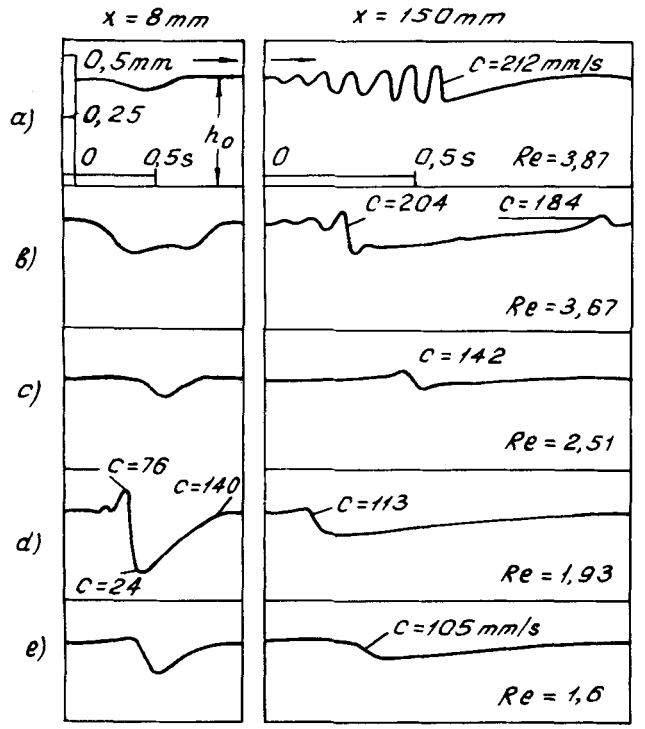

Figure 21. Evolution of negative disturbances.

$\nu = 7.8 \cdot 10^{-6}$ m²/s; $\sigma/\rho = 56.7 \cdot 10^{-6}$ m³/s².

Here $U^* = gh^{*2}/3\nu$. In the case of the wave step, the mean film thickness beyond the wave front was taken as h^*. Thus, as follows from the analysis of the given results, the square nonlinearity alone is not sufficient to adequately describe the steps in the wave propagation differential equations.

The evolution of the localized positive disturbances is shown in Figure 20. Here the characteristic value of the disturbance Reynolds number $Re^* = gh^{*3}/3\nu^2$ has been plotted according to the maximum thickness of the initial disturbance. At low Re and Re^*, gradual steepening of the leading wave front occurs and the waveform assumes the triangular nonsymmetric shape (the Bürger triangle type). Later on, the width of the disturbance grows and the amplitude decreases. The triangular wave velocity determined according to the leading front roughly corresponds to the velocity of the steps whose amplitude is the same. This can be accounted for by the fact that the trailing front is very gently sloping and long, therefore the flow therein is locally in equilibrium, as with the region beyond the front of the step. The tail of the wave must propagate at the velocity of an infinitely long linear disturbance which is equal to $3 \cdot U_o$.

At $Re^* > Re_*$ (in this case, $Re_* \approx 3$), the break of the initial solitary disturbance occurs, whereby a train of periodic or solitary waves is formed (Figure 20b). Since $Re^* > Re_*$ and the initial disturbance is rather long (50–100), the break is due to the same mechanism as with the wave formation on a smooth film, i.e., it is due to the hydrodynamic instability. In the case of the long initial disturbance, the number of waves formed as a result of the break can be estimated according to the fastest-growing-waves linear theory.

As can be seen from the oscillograms in Figure 20b, first of all the waves in the leading part of the initial disturbance are formed, evolving, similarly, into the waves that naturally develop on a smooth film (Figure 7). As fast as the wave packet is formed, the waves become nonlinear and their velocity begins to depend on their amplitude. As with the sequence of the stationary solitary waves (Figures 13a and 15a), the velocity of the solitary waves in the train turns out to also be proportional to their amplitude, which is shown in Figure 19. However, as a whole the wave formation picture is quasistationary. It is connected both with the difference in the velocities of separate waves, as well as with the fact that a stationary wave of certain amplitude can exist with an appropriate, rigorously determined thickness only. If a solitary wave of smaller amplitude goes ahead of a wave of greater amplitude, then due to the difference in the propagation velocities, nonlinear interaction with a newly formed solitary wave, propagating at an even greater velocity, ultimately occurs. Such a process considerably differs from the interaction between solitons, i.e., solitary waves which can be described by the Korteveg-de Vries equation.

Negative localized disturbances are always essentially nonstationary (Figure 21), i.e., their wave characteristics undergo noticeable alterations at distances whose order is that of the length of the disturbance. They evolve similarly into triangular positive disturbances.

NOTATION

A = particle track spacing
a = $h_{max} - h_{min}$
C = phase velocity
C_o = $3U_o$
C_1 = $1.69\ U_o$
C_2 = $0.71\ U_o$
f = frequency
$f(\eta)$ = function in the velocity profile expression
Fi = film number, $\sigma^3/\rho^3 g\nu^4$
g = gravitational acceleration
H = h'/h_o
h = film thickness
h_o = smooth laminar film thickness
k = wave number, $2\pi h_o/\lambda$
L = characteristic longitudinal scale
N = magnification
n = refraction
P = pressure
q = instantaneous volume liquid flow rate per unit width of a film
q_o = mean flow rate
Re = Reynolds number, q_o/ν
t = time
U = longitudinal component of surface velocity
u,v = longitudinal and transverse velocity components
We = Weber number, $\sigma/\rho g h_o^2$
x,y = longitudinal and transverse coordinates

Greek Letters

$-\alpha$ = spatial growth rate factor of amplitude
β = temporal growth rate
$\gamma,\delta,æ,\chi$ = coefficients in Eq. 17
ϵ = long-wave process parameter, h_o/λ
ϵ_1 = amplitude disturbance parameter
$\zeta\eta$ = y/h
θ = angular coordinate
λ = wavelength
ν = kinematic viscosity
ξ = x-Ct
ρ = liquid density
σ = liquid surface tension
ϕ = function in Eq. 37
Ω = dimensionless complex frequency, $\Omega = \omega + i\beta$
ω = real part of Ω

Subscripts

R	= values relating to residual layer
max	= maximum value
min	= minimum value
*	= critical value

Superscripts

$'$	= disturbed part of a value
$-$	= value made dimensionless by using L and u_o
$\sim$	= value made dimensionless by using h_o and u_o
*	= value of thickness (velocity, Re number) beyond the front of initial solitary disturbance

LITERATURE CITED

Anshus, B. E., "On the Asymptotic Solution to the Falling Film Stability Problem," *Ind. and Eng. Chem. Fund.*, **11**, 502 (1972).

Benjamin, T. B., "Wave Formation in Laminar Flow Down an Inclined Plane," *J. Fluid Mech.*, **2**, 554 (1957).

Benney, D. J., "Long Waves on Liquid Films," *J. Math. and Phys.*, **45**, 150 (1966).

Cook, R. A., and R. H. Clark, "The Experimental Determination of Velocity Profiles in Smooth Falling Liquid Films," *Can. J. Chem. Eng.*, **49**, 412 (1971).

Ganchev, B. G., V. M. Kozlov, and V. V. Orlov, "Some Results of Falling Liquid Film Studies by Stroboscopic Visualization Technique," *Zh. Prikl. Mekh. Tekh. Fiz.*, **2**, 140 (1972).

Gjevik, B., "Occurrence of Finite-Amplitude Surface Waves on Falling Liquid Films," *Phys. Fluids*, **13**, 1,918 (1970).

Ivanilov, Yu. P., "Roll Waves in Inclined Channels," *Zh. Vych. Mat. i Mat. Fiz.*, **1**, 1,061 (1961).

Jones, L. O., and S. Whitaker, "An Experimental Study of Falling Liquid Films," *AIChE J.*, **12**, 525 (1966).

Kapitza, P. L., "Wave Flow of Thin Viscous Liquid Films," *Zh. Exper. i Teor. Fiz.*, **18**, 3 (1948).

Kapitza, P. L., and S. P. Kapitza, "Wave Flow of Thin Viscous Liquid Films," *Zh. Exper. i Teor. Fiz.*, **19**, 105 (1949).

Krylov, V. S., V. P. Vorotilin, and V. G. Levich, "Theory of Wave Flow of Thin Liquid Films," *Teor. Osnovy Khim. Tekhnol.*, **3**, 499 (1969).

Krantz, W. B., and S. L. Goren, "Stability of Thin Liquid Films Flowing Down a Plane," *Ind. and Eng. Chem. Fund.*, **10**, 91 (1971).

"Lee J. Kapitza's Method of Film Flow Description," *Chem. Eng. Sci.*, **24**, 1,309 (1969).

Maurin, L. N., G. E. Odishariya, and A. A. Tochigin, "Solitary Waves on a Falling Liquid Film," *Nonlinear Wave Processes in Two-Phase Media*, S. S. Kutateladze, Ed., Inst. Thermophysics, Novosibirsk, 190 (1977).

Nakoryakov, V. E., and I. R. Shreiber, "Surface Waves on Thin Liquid Films," *Zh. Prikl. Mekh. Tekh. Fiz.*, **2**, 109 (1973).

Nakoryakov, V. E., et al., "Flows of Thin Liquid Films," *Wave Processes in Two-Phase Systems*, S. S. Kutateladze, Ed., Inst. Thermophysics, Novosibirsk, 129 (1975).

Nakoryakov, V. E., B. G. Pokusaev, and S. V. Alekseenko, "Stationary Two-Dimensional Roll Waves on Vertical Falling Liquid Films," *JEP (Soviet J. of Engineering Physics)*, **30**, 780 (1976).

Nakoryakov, V. E., et al., "Instantaneous Velocity Profiles in a Wave Liquid Film," *JEP*, **33**, 399 (1977).

Nepomnyashchii, A. A., "Wave Regime Stability in a Film Falling Down Inclined Surfaces," *Izv. Akad. Nauk SSSR, Ser. Mekh. Zhidk. i Gaza*, **3**, 28 (1974).

———, "Wave Motion Stability in a Layer of Viscous Liquid on Inclined Surfaces," *Nonlinear Wave Processes in Two-Phase Media*, S. S. Kutateladze, Ed., Inst. Thermophysics, Novosibirsk, 181 (1977).

Pashinina, L. V., "Steady-State Flows in Thin Films," *Izv. Akad. Nauk SSSR, Mekh. Zhidk. i Gaza*, **3**, 173 (1966).

Petviashvili, V. I., and O. Yu. Tzvelodub, "Horseshoe Solitons on Falling Viscous Liquid Films," *Dokl. Akad. Nauk SSSR*, **238**, 1,321 (1978).

Pierson, F. W., and S. Whitaker, "Some Theoretical and Experimental Observations of the Wave Structure of Falling Films," *Ind. and Eng. Chem. Fund.*, **16**, 401 (1977).

Pokusaev, B. G., and S. V. Alekseenko, "Two-Dimensional Waves on Vertical Falling Liquid Films," *Nonlinear Wave Processes in Two-Phase Media*, S. S. Kutateladze, Ed., Inst. Thermophysics, Novosibirsk, 158 (1977).

Portalski, S., and A. J. Clegg, "An Experimental Study of Wave Inception on Falling Liquid Films," *Chem. Eng. Sci.*, **27**, 1,257 (1972).

Shkadov, V. Ya., "Wave Flows of Thin Viscous Liquid Films Under the Gravity Force Action," *Izv. Akad. Nauk SSSR, Mekh. Zhidk. i Gaza*, **1**, 43 (1967).

———, "Some Problems of the Theory of Wave Flows of Thin Viscous Liquid Films," *Izv. Akad. Nauk SSSR, Mekh. Zhidk. i Gaza*, **2**, 20 (1968).

———, "Some Methods and Problems of Theory of Hydrodynamic Stability," *Proc.*, No. 25, Inst. Mekh. MGU, Moskva (1973).

Strobel, W. J., and S. Whitaker, "The Effects of Surfactants on the Flow Characteristics of Falling Liquid Films," *AIChE J.*, **15**, 527 (1969).

Tzvelodub, O. Yu., "Stationary Running Waves on a Film Falling Down Inclined Surfaces," *Izv. Akad. Nauk SSSR, Mekh. Zhidk. i Gaza*, **4** (1980).

Whitham, G. B., *Linear and Nonlinear Waves*, Wiley, New York (1974).

Whitaker, S., "Effect of Surface Active Agents on the Stability of Falling Liquid Films," *Ind. and Eng. Chem. Fund.*, **3**, 132 (1964).

Manuscript received Aug. 22, 1980; revision received Oct. 12 and accepted Oct. 29, 1984.